Impact of Light Illumination and Passivation Layer on Silicon Finite-Ground Coplanar-Waveguide Transmission-Line Properties

Solon J. Spiegel, *Associate Member, IEEE,* and Asher Madjar, *Fellow, IEEE*

***Abstract*—Modeling of silicon finite-ground coplanar-waveguide (FGCPW) transmission lines is presented in this paper. It is shown that the effective substrate conductivity increases in the presence of illumination and in the presence of a passivation layer in the slot regions independently. As a result, the losses of trenched FGCPW are lower than conventional FGCPW transmission lines. The strong dependence of the substrate conductivity on illumination suggests that optically controlled attenuators can be implemented with FGCPW transmission lines exhibiting practically no phase change between the different attenuation states. A new contrast ratio for optically controlled transmission lines is derived.**

***Index Terms*—Coplanar waveguides, silicon substrates, transmission lines.**

I. Introduction

STRINGENT cost, size, power consumption, and performance demanded from modern commercial and military systems have led to rapid advances in the areas of monolithic microwave integrated circuits (MMICs) [1], [2], RF micro-electromechanical devices (RFMEMs) [3], [4], and microwave packaging [5]–[8] technologies. The high level of integration of analog and digital circuits and the off-chip elements has shifted the conventional design approach, where each subsystem is designed separately, to a more unified approach for systems, circuit, and packaging. In such a dense environment, it is very difficult to take into account the interaction between the different elements of a module (MMICs, application-specific integrated circuits (ASICs), shield, interconnects, etc.), particularly when multiple technologies are employed. As a result, the actual system performance is different from the predicted system performance based on wafer measurements data.

Hybrid integration of active devices on high-resistivity silicon substrates offers an attractive cost/performance solution for microwave subsystems. For instance, Ramam *et al.* [9] shows a subharmonic mixer designed at 94 GHz and Sakay *et al.* [10] describes a single stage amplifier at 40 GHz. In addition, silicon substrates provide the means (optical benches) of conveying the optical signals. The use of optical techniques for the control of microwave circuits has been described in [11]–[14]. A gain control up to 45 dB using a commercial AlGaAs laser diode is demonstrated in [12].

Coplanar-waveguide (CPW) transmission lines have been recently recognized as a preferable propagation medium at millimeter-wave frequencies in comparison with the commonly used microstrip lines. The dispersion characteristics of CPW lines are analyzed in [15]–[18]. One of the main advantages of a CPW transmission line and its variations (CPW [16], trenched finite-ground coplanar waveguide (FGCPW) [19], finite-ground coplanar (FGC) [20], conductor-backed CPW [21], quasi-CPW [22]) is the ability to support small and low-cost packages. The existence of an upper ground plane allows a straightforward integration between the flip-chip devices and the mounting substrate. The strong electric-field confinement at the slot areas in high aspect-ratio CPW lines reduces the propagation of undesirable non-TEM modes. As a result, CPW lines present lower dispersion characteristics and higher isolation between adjacent elements than microstrip lines. On the other hand, at relatively lower frequencies, where the main loss contributor stems from the conductor losses, CPW lines are expected to have higher losses per wavelength. The losses CPW transmission lines, however, can be somewhat reduced by a reduction in the circuit size due to an improvement in the isolation between adjacent elements.

High thermal conductivity and low dielectric-loss substrates are the key parameters in CPW-based circuits. Unlike microstrip circuits, where the heat flows through the substrate and via holes to a high thermal conductivity carrier, e.g., molybdenum, the heat sink in CPW structures is mainly determined by the thermal conductivity of the substrate as well as by the thermal and electrical properties of the interconnects. Substrates, such as silicon, present a reasonable compromise between losses and thermal conductivity. The thermal conductivity of silicon is approximately 150 W/mK. The losses of a CPW transmission line on a high-resistivity silicon substrate (HRSS) lower than 0.2 dB/mm at 40 GHz [23] are considered acceptable for most of the microwave and the millimeter-wave applications.

Silicon FGCPW transmission lines require the presence of a passivation layer between the metal lines and the substrate to avoid the formation of Schottky junctions. Silicon nitride, as well as silicon dioxide, is a viable insulating candidate. The charges accumulated at the interface, the existent traps in the passivation layer, and the interface trapped charges cause an increase of the effective substrate conductivity and, in turn, of the dielectric losses. Since most of the electric field is confined at the slot-area CPW lines, removing the passivation layer from

Manuscript received May 19, 2000.

S. J. Spiegel is with the Intel Cellular Communication Division, Digital Signal Processing Communications (DSPC), Givat Shmuel 51905, Israel (e-mail: solon.spiegel@dspis.co.il).

A. Madjar is with RAFAEL 87, 31021 Haifa, Israel.

Publisher Item Identifier S 0018-9480(00)08730-5.

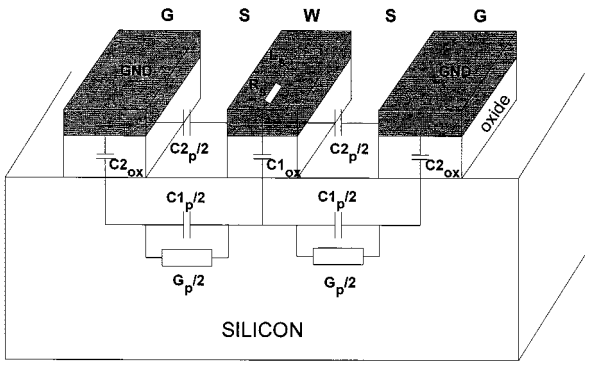

Fig. 1. Cross section of a trenched FGCPW transmission line.

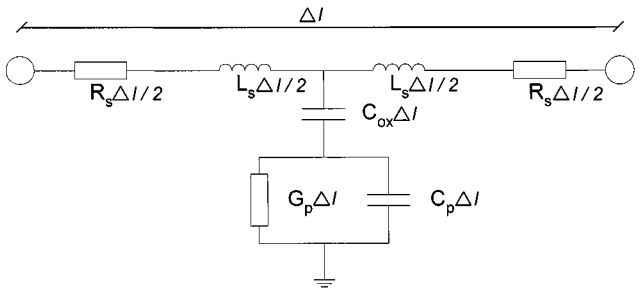

Fig. 2. FGCPW differential transmission line.

the slot areas leads to a reduction of the surface charge. Analytical transmission line models for lossy silicon substrates are described in [25] and [26].

In this paper, the dependence of the substrate conductivity on the passivation layer is investigated for silicon FGCPW transmission lines. Section II describes the differential transmission-line equivalent model and its dependence on the passivation layer. The influence of the illumination on the differential transmission-line equivalent model is analyzed. The results show that the effective substrate conductivity varies according to the light illumination and to the surface charges at the slot areas. Finally, the amplitude and phase of the insertion and return losses of silicon FGCPW transmission lines are presented. It will be shown that, at frequencies above 1 GHz, silicon FGCPW transmission lines act as an optically controlled variable attenuator having phase linear with frequency. The linear phase characteristics of FGCPW transmission lines enables the appearance of new applications such as gain control at microwave and millimeter-wave frequencies for phase tracking systems, automatic gain control, power control device for transmitter modules, and temperature control devices.

II. Transmission-Line Modeling

The cross section of the trenched FGCPW transmission-line structure considered in this paper is shown in Fig. 1. W is the width of the signal line, S is the width of the slot, and G is the width of ground lines. The capacitance $C1_{\rm ox}$ and $C2_{\rm ox}$ stand for the capacitance of the oxide layer under the signal and ground lines, respectively. The capacitance $C1_p$ and $C2_p$ represent the capacitance between the signal and ground lines of CPW structures. The signal-to-ground coupling through the substrate is given by $C1_p$ and through the air dielectric by $C2_p$. The substrate conductivity and influence of surface charge are taken into account by the shunt conductance G_p. The series elements R_s and L_s describe the resistance and self-inductance of the center conductor line. The capacitance is expressed in picofarads/millimeters, the inductance in henries/millimeters, the resistance in ohms/millimeters, and the conductance in siemens/millimeters.

The difference between the trenched FGCPW model in Fig. 1 and the conventional FGCPW model is that, in the latter, the oxide layer stretches over the slot regions. In this paper, we will designate the trenched FGCPW transmission line by T-FGCPW and the conventional FGCPW transmission line simply by FGCPW.

In order to reduce the complexity of the transmission-line model, the ground plane is considered large enough to neglect the influence of the oxide layer underneath the ground metal layer, i.e., $C2_{\rm ox} \to \infty$. This assumption is justified for most of CPW designs, where the ground plane is set to at least twice the distance between the ground lines to reduce the effect of a finite-width ground plane on the characteristic impedance.

Fig. 2 shows the simplified differential transmission-line equivalent model. The signal-to-ground capacitance $C1_p$ and $C2_p$ are represented by a single capacitance C_p. The T-type equivalent transmission-line model can be applied to analyze the dependence of the transmission-line parameters on the passivation layer and on the light illumination at low frequencies, i.e., at $\Delta l \ll \lambda/4$.

In our experiments, the length of the silicon T-FGCPW and FGCPW (Δl) equals 5000 μm and the dimensions W, S, and G, as shown in Fig. 1, equal $W = 75$ μm, $S = 52$ μm, and $G = 360$ μm. The transmission-line parameters were extracted from the z-matrix representation of the transmission line at frequencies below 1 GHz where $\Delta l < \lambda/24$.

The series transmission-line parameters $R_s\Delta l$ and $L_s\Delta l$ are given by

$$R_s\Delta l = \mathrm{Re}\,(Z_{11} + Z_{22} - 2Z_{21}) \tag{1}$$

$$L_s\Delta l = \frac{1}{\omega}\,\mathrm{Im}\,(Z_{11} + Z_{22} - 2Z_{21}) \tag{2}$$

where $\omega = 2\pi f$.

The equivalent shunt elements $G_{\rm eq}\Delta l$ and $C_{\rm eq}\Delta l$ are expressed in terms of $G_p\Delta l$, $C_p\Delta l$, $C_p\Delta l$, and $C_{\rm ox}\Delta l$ by

$$G_{\rm eq}\Delta l = G_p\left(\frac{C_{\rm ox}}{C_{\rm ox}+C_p}\right)^2\Delta l \cong \mathrm{Re}\left(\frac{1}{Z_{21}}\right) \tag{3}$$

$$C_{\rm eq}\Delta l = \frac{C_{\rm ox}C_p}{C_{\rm ox}+C_p}\Delta l \cong \frac{1}{\omega}\,\mathrm{Im}\left(\frac{1}{Z_{21}}\right). \tag{4}$$

Equations (3) and (4) are valid for $G_p\Delta l \ll \omega C_p\Delta l$. The value of $C_{\rm ox}\Delta l$ must account for the capacitance of the region underneath the center conductor line and for the fringe capacitance. The latter contribution is particular relevant for small-signal linewidth of a CPW transmission line. The value of $C_{\rm ox}\Delta l$ can be calculated by

$$C_{\rm ox}\Delta l = \left(\frac{W}{T_{\rm ox}}\varepsilon_{\rm ox}\varepsilon_o + C_{\rm fringe}\right)\Delta l \tag{5}$$

where W is the width of center conductor line, $T_{\rm ox}$ is the thickness of the oxide region, $\varepsilon_{\rm ox}$ is the dielectric constant of the oxide layer, and $\varepsilon_o = 8.854 \times 10^{-14}$ F/cm. The fringe capacitance $C_{\rm fringe}$ is written as [26]

$$C_{\rm fringe} = \varepsilon_{\rm reff}\varepsilon_0 \left(\frac{2\pi}{\ln(1+T+\sqrt{T(T+2)})} - \frac{1}{T} \right) \quad (6)$$

where $T = 2T_{\rm ox}/t$ and t is the thickness of the metal layer. The value of $C_{\rm ox}\Delta l$ can also be determined from $\lim_{\omega\to 0}\ [\omega^{-1}\ \mathrm{Im}(Z_{21})^{-1}]$.

The influence of the passivation layer and the light illumination on the transmission-line losses is investigated for the T-FGCPW and FGCPW transmission lines. We analyze the following four different cases:

1) FGCPW not illuminated;
2) FGCPW illuminated;
3) T-FGCPW not illuminated;
4) T-FGCPW illuminated.

In our experiment, a white light source was positioned at a distance of 3 cm away from the surface of the substrate. The spot size on the sample is 900 μm $\times$ 5000 μm, i.e., $(2S+2G+W)\times L$. Due to the nature of the light source, most of the energy was wasted by not impinging on the slot areas $(S \times L)$ of the FGCPW structures. On-wafer s-parameters of T-FGCPW and FGCPW transmission lines were measured with the light source switched on and off. The results provide a qualitative rather than quantitative estimate of the dependence of the transmission-line properties on the optical power density at the sample.

Fig. 3(a) shows that $R_s\Delta l$ depends neither on the illumination, nor on the passivation layer. In other words, the conductor loss is insensitive to the light illumination and to the presence of the passivation layer.

Fig. 3(b) shows the dependence of the equivalent substrate conductivity $(G_{\rm eq}\Delta l)$ on the light illumination and passivation layer. Under illumination, the substrate losses increase due to the increase of the effective substrate conductivity. A comparison between T-FGCPW and FGCPW transmission lines indicates that the removal of the oxide layer causes a reduction in the substrate losses. The variation in the effective substrate conductivity can be explained by the accumulation, inversion, and depletion of charges at the Si–SiO_2 interface, by the variation of the interface trapped charges, and by the charges located in the SiO_2 region.

Finally, Fig. 4(a) and (b) show the real and imaginary parts of the characteristic impedance of silicon T-FGCPW and FGCPW transmission lines. At low frequencies, the characteristic impedance is strongly dependent on the substrate losses. In either the absence of illumination or at high frequencies, the loss quantities $G_{\rm eq}\Delta l$ and $R_s\Delta l$ are much smaller than the reactive terms $L_s\Delta l$ and $C_p\Delta l$. Thus, above 10 GHz, the characteristic impedance can be approximated by the characteristic impedance of a lossless transmission line [27]

$$L_s\Delta l \approx C_p\Delta l Z_o^2. \quad (7)$$

Table I summarizes the extracted values of the series resistance and the effective shunt conductivity for the four cases analyzed below 1 GHz. The values of $C_{\rm ox}\Delta l$, $C_p\Delta l$, and $L_s\Delta l$ are 129 pF, 0.8 pF, and 1.8 pH, respectively. The propagation constant remains unchanged for the different values of the substrate conductivity, as described in the Section IV.

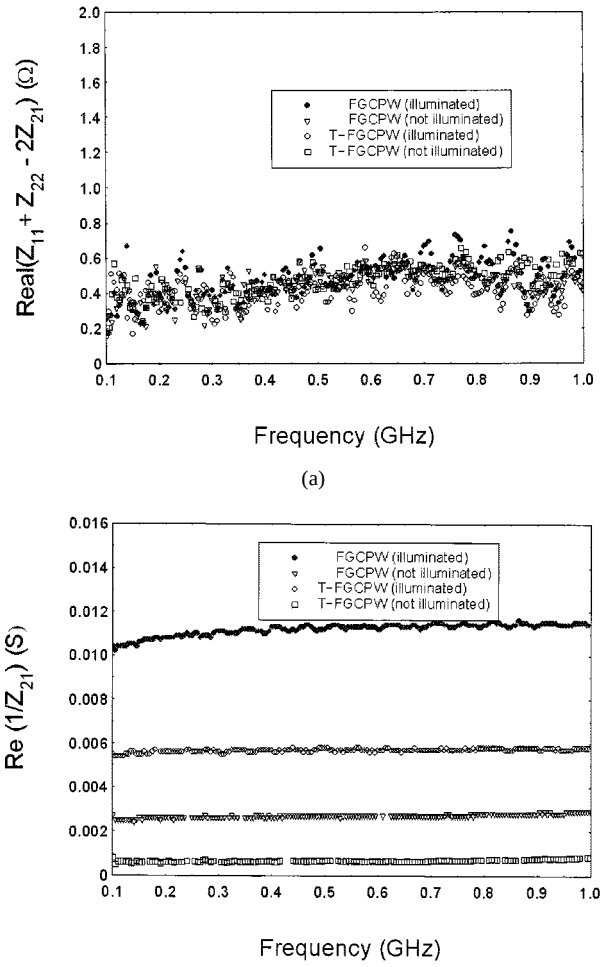

Fig. 3. (a) $\mathrm{Real}(Z_{11}+Z_{22}-2Z_{21})$ versus frequency. (b) $\mathrm{Re}(1/Z_{21})$ versus frequency.

III. Fabrication

A 1000-A SiO_2 layer was thermally grown on the surface of a 330-μm-thick high-resistivity silicon substrate ($\rho \cong 1200\ \Omega\ \cdot$ cm). A composite layer, i.e., Ni-Cr-Au, with thickness equals 5000 A, was then deposited on the surface of the oxide and covered with photo-resist. Following the definition of the exposed regions, a 2.5-μm-thick galvanic gold metal was formed using electroplating techniques. Finally, the SiO_2 layer was etched down using a buffered oxide etch (BOE) solution. The low etching rate enabled the trenches to be formed while minimizing the undercutting and not degrading the line metallization. No metal was deposited on the backside surface.

IV. Results

Fig. 5 presents the return losses of the 5000-μm silicon T-FGCPW and FGCPW transmission lines. At low frequencies, the characteristic impedance depends upon the value of the

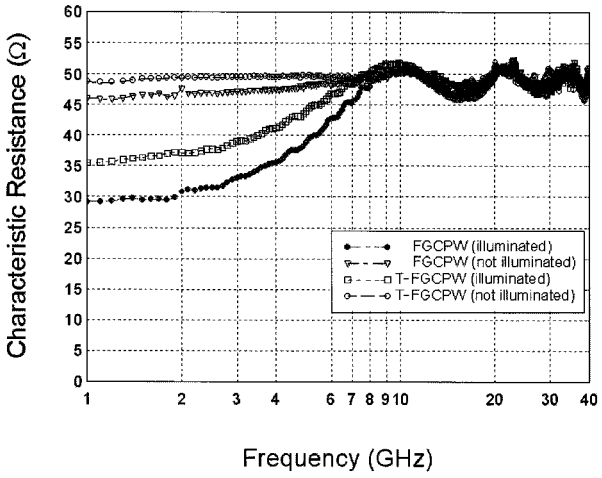

(a)

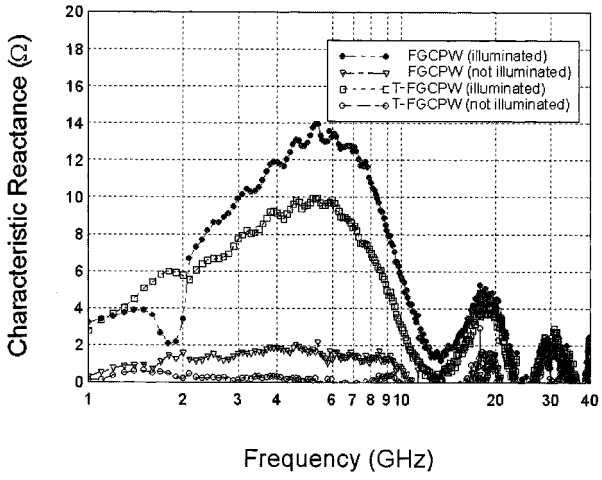

(b)

Fig. 4. (a) Characteristic resistance versus frequency. (b) Characteristic reactance versus frequency.

TABLE I
SUMMARY OF THE EXTRACTED TRANSMISSION-LINE LOSSES

	$R_s\Delta l$ (Ω)	$G_{eq}\Delta l$ (S)
T-FGCPW not illuminated	0.4	0.00067
T-FGCPW illuminated	0.4	0.00580
FGCPW not illuminated	0.4	0.00267
FGCPW illuminated	0.4	0.01120

effective conductivity. Owing to its high value in the presence of the light illumination, the refection coefficient is large at low frequencies. At high frequencies, however, the effective shunt conductance does not contribute to the reflection coefficient, i.e., the characteristic impedance can be expressed solely as a function of $L_s\Delta l$ and $C_p\Delta l$. From Fig. 5, it is seen that S_{11} is practically the same for all the cases at frequencies above 20 GHz.

The plot of S_{21} and the attenuation (decibels/centimeters) of T-FGCPW and FGCPW transmission lines are shown in Figs. 6 and 7, respectively. The attenuation of the transmission lines increases by approximately the same amount of the effective substrate conductivity, indicating that the dielectric loss is the predominant loss in the presence of the illumination.

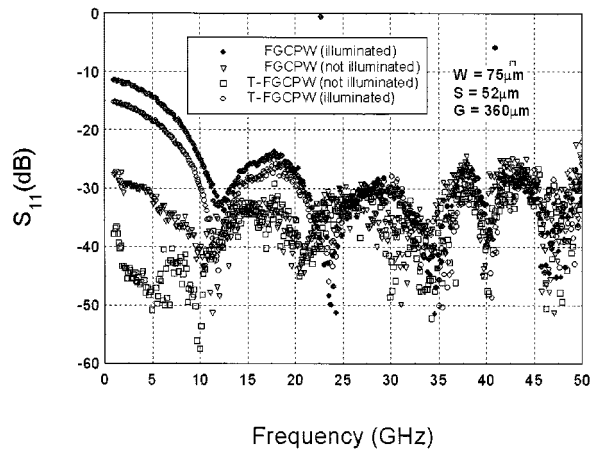

Fig. 5. Return loss of FGCPW transmission lines.

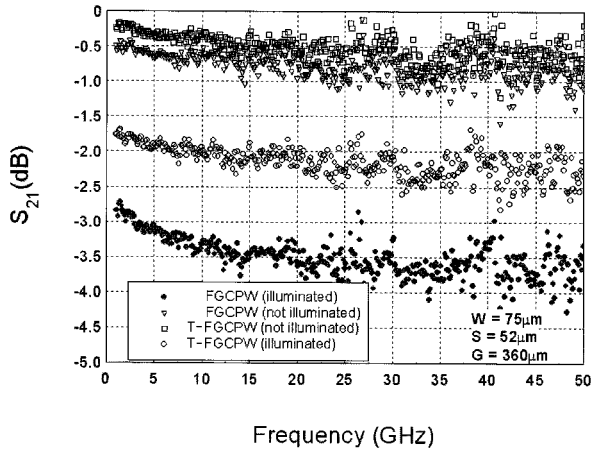

Fig. 6. Insertion loss of FGCPW transmission lines.

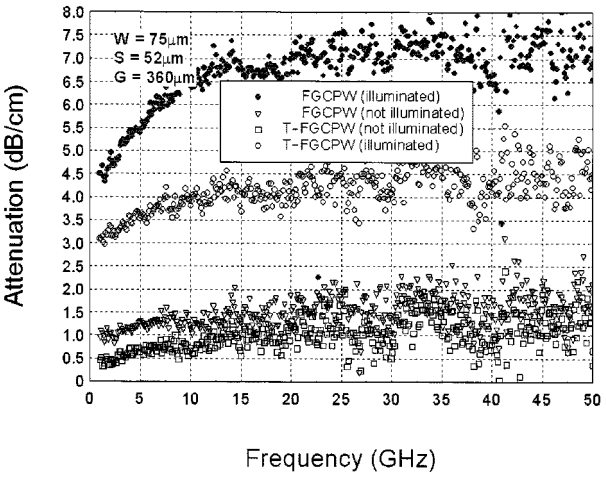

Fig. 7. Attenuation of FGCPW transmission lines.

TABLE II
CONDUCTOR LOSS, DIELECTRIC LOSS, AND CONTRAST RATIO OF SILICON FGCPW AND T-FGCPW TRANSMISSION LINES

	Conductor loss factor (mm^{-1})	Dielectric loss factor (mm^{-1})	C.R.
T-FGCPW not illuminated	0.0008	0.0034	
T-FGCPW illuminated	0.0008	0.0290	6.1
FGCPW not illuminated	0.0008	0.0134	
FGCPW illuminated	0.0008	0.0560	3

The effective dielectric loss factor (mm^{-1}) is expressed by

$$\alpha_d = \frac{1}{2}(G_{\text{eff}} Zc) \tag{8}$$

and

$$G_{\text{eff}} = \frac{\varepsilon_i}{\varepsilon_r}\omega\varepsilon_{\text{Si}}\varepsilon_o + G_p\left(\frac{G_{\text{ox}}}{C_{\text{ox}}+C_p}\right)^2$$

where $\varepsilon = \varepsilon_r + j\varepsilon_i$ and $\varepsilon_{\text{Si}}\varepsilon_o$ is the permittivity of the silicon substrate. The second term of the effective substrate conductivity indicates that the effective dielectric loss varies with the intensity of the light illumination. The extraction of $G_{\text{eq}}\Delta l$ with and without illumination was shown in Fig. 3(b).

The conductor loss factor (mm^{-1}) is expressed by

$$\alpha_c = \frac{1}{2}\left(\frac{R_s}{Zc}\right) \tag{9}$$

and

$$R_s\Delta l = \left[\sigma_c\delta\tanh\left(\frac{t}{\delta}\right)\right]^{-1}$$

where σ_c is the metal conductivity, δ is the skin depth, and t is the metal thickness. Table II outlines the conductor and dielectric losses and the contrast ratio (CR) for optically controlled devices. The strong dependence of dielectric loss of silicon substrates on illumination allows silicon T-FGCPW and FGCPW transmission lines to be used as optically controlled devices. A new CR for optically controlled transmission-line devices can be defined in terms of the conductor and dielectric losses by

$$\text{CR} = \left(\frac{a_{d(\text{n.ill.})}}{a_{d(\text{n.ill.})}+a_c}\right)\left(\frac{a_{d(\text{ill.})}}{a_{d(\text{n.ill.})}}-1\right) \tag{10}$$

where the indexes ill. and n.ill. stand for illuminated and nonilluminated, respectively.

Table II outlines the conductor and dielectric losses for the four cases analyzed and the CR of the FGCPW and T-FGCPW transmission lines. The CR of the T-FGCPW was found higher than FGCPW transmission lines for optically controlled devices due to: 1) low conductor loss in comparison with the dielectric loss and 2) to the higher ratio between illuminated and nonilluminated dielectric losses.

The insertion phase at frequencies above 1 GHz is neither sensitive to illumination, nor to the passivation layer, as shown in Fig. 8. This is justified by the fact that the propagation constant (β) is weakly dependent on the equivalent substrate conductivity since $R_sG_{\text{eq}} \ll \omega^2 L_s C_{\text{eq}}$. The removal of the 1000-A oxide layer from the slot regions does not alter the value of the effective dielectric constant. This is not valid, however, for deep trenches where the effective dielectric constant varies according to the depth of the trench [22].

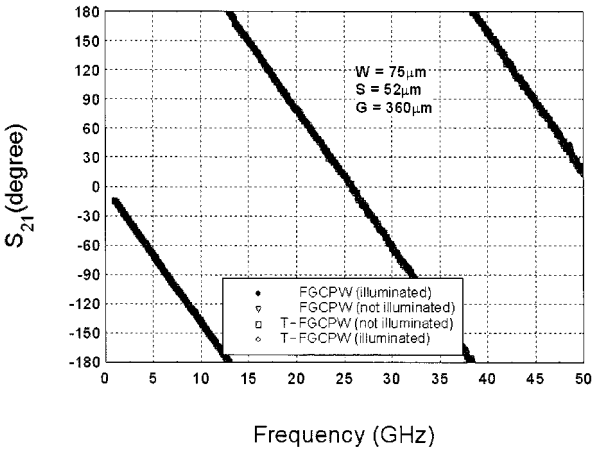

Fig. 8. Insertion phase of FGCPW transmission lines.

One of the possible applications of these devices is in the area of an optically controlled wide-band attenuator when small phase errors for the different levels of attenuation are required. For instance, in a complete millimeter-wave monopulse receiver unit in which the phase tracking between channels is crucial, a silicon transmission line can be placed between the transmitter/receiver (T/R) switch and the low-noise amplifier (LNA) stages to improve the system dynamic range and to avoid driving the LNA into the nonlinear regime. The low phase error in comparison with either p-i-n or pseudomorphic high electron-mobility transistor (pHEMT) attenuators ensures the phase tracking between monopulse channels.

V. CONCLUSION

We have presented the effect of the light illumination and the passivation layer on the silicon FGCPW transmission lines. In the presence of illumination, the effective substrate conductivity increases, leading to an increase in the dielectric losses. The losses of T-FGCPW, due to the removal of the oxide layer from the slot regions, are smaller than the losses in conventional FGCPW. The strong dependence of the effective substrate conductivity on illumination suggests that silicon FGCPW transmission lines can be applied for implementing wide-band microwave and millimeter-wave optically controlled variable at-

tenuators having low phase errors for the different levels of attenuation.

REFERENCES

[1] H. Tserng *et al.*, "Embedded transmission line (ETL) MMIC for low-cost, high-density wireless communication applications," in *IEEE Radio Freq. Integrated Circuits Symp. Dig.*, Denver, CO, June 1997, pp. 41–44.

[2] B. Agarwal *et al.*, "80-GHz distributed amplifiers with transferred-substrate heterojunction bipolar transistors," *IEEE Trans. Microwave Theory Tech.*, vol. 46, pp. 2302–2307, Dec. 1998.

[3] C. L. Goldsmith *et al.*, "Performance of low-loss RF MEMS capacitive switches," *IEEE Microwave Guided Wave Lett.*, vol. 8, pp. 269–271, Aug. 1998.

[4] E. R. Brown, "RF-MEMS switches for reconfigurable integrated circuits," *IEEE Trans. Microwave Theory Tech.*, vol. 46, pp. 1868–1880, Nov. 1998.

[5] T. A. Midford *et al.*, "The evolution of packages for monolithic microwave and millimeter-wave circuits," *IEEE Trans. Antennas Propagat.*, vol. 43, pp. 983–991, Sept. 1995.

[6] K. J. Herrick *et al.*, "Microtechnology in the development of three-dimensional circuits," *IEEE Trans. Microwave Theory Tech.*, vol. 46, pp. 1832–1844, Nov. 1998.

[7] M. I. Herman *et al.*, "Novel techniques for millimeter-wave packages," *IEEE Trans. Microwave Theory Tech.*, vol. 43, pp. 1516–1523, July 1995.

[8] R. F. Drayton *et al.*, "Development of self-packaged high frequency circuits using micromachining techniques," *IEEE Trans. Microwave Theory Tech.*, vol. 43, pp. 2073–2080, Sept. 1995.

[9] S. Ramam *et al.*, "A high-performance W-band uniplanar subharmonicmixer," *IEEE Trans. Microwave Theory Tech.*, vol. 45, pp. 955–962, June 1997.

[10] H. Sakai *et al.*, "A novel millimeter-wave IC on Si substrate using flip-chip bonding technology," *IEICE Trans. Electron.*, vol. E78-C, no. 8, pp. 971–978, Aug. 1995.

[11] S. E. Saddow *et al.*, "An optoelectronic attenuator for the control of microwave circuits," *IEEE Microwave Guided Wave Lett.*, vol. 3, pp. 361–362, Oct. 1993.

[12] S. E. Saddow and C. H. Lee, "Scattering parameter measurements on an optoelectronic attenuator," in *IEEE MTT-S Int. Microwave Symp. Dig.*, San Diego, CA, 1994, pp. 1383–1386.

[13] S. E. Saddow and C. H. Lee, "Optical control of microwave integrated circuits using high-speed GaAs and Si photoconductive switches," *IEEE Trans. Microwave Theory Tech.*, vol. 43, pp. 2414–2420, Sept. 1995.

[14] S. J. Spiegel and A. Madjar, "Light dependence of silicon FGCPW transmission lines," in *IEEE MTT-S Int. Microwave Symp. Dig.*, Anaheim, CA, 1999, pp. 1801–1804.

[15] M. Y. Frankel *et al.*, "Terahertz attenuation and dispersion characteristics of coplanar transmission lines," *IEEE Trans. Microwave Theory Tech.*, vol. 39, pp. 910–916, June 1991.

[16] M. Riaziat *et al.*, "Propagation modes and dispersion characteristics of coplanar waveguides," *IEEE Trans. Microwave Theory Tech.*, vol. 38, pp. 2543–2554, Mar. 1990.

[17] G. Hasnain *et al.*, "Dispersion of picosecond pulses in coplanar transmission lines," *IEEE Trans. Microwave Theory Tech.*, vol. 34, pp. 738–741, June 1996.

[18] H. Cheng *et al.*, "Terahertz-bandwidth characterization of coplanar transmission lines on low permittivity substrates," *IEEE Trans. Microwave Theory Tech.*, vol. 42, pp. 2399–2406, June 1994.

[19] S. Yang *et al.*, "Characteristics of trenched coplanar waveguide for high-resistivity Si MMIC applications," *IEEE Trans. Microwave Theory Tech.*, vol. 46, pp. 623–631, May 1998.

[20] K. T. Herrick *et al.*, "W-band micromachined finite ground coplanar (FGC) line circuit elements," in *IEEE MTT-S Int. Microwave Symp. Dig.*, Denver, CO, 1997, pp. 269–272.

[21] W.-T. Lo *et al.*, "Resonant phenomena in conductor-backed coplanar waveguide (CBCPW)," in *IEEE MTT-S Int. Microwave Symp. Dig.*, 1993, pp. 1199–1202.

[22] A. Reichelt and I. Wolff, "New coplanar-like transmission lines for applications in monolithic integrated millimeter-wave and submillimeter-wave circuits," in *IEEE MTT-S Int. Microwave Symp. Dig.*, Baltimore, MD, 1998, pp. 99–102.

[23] G. E. Ponchak *et al.*, "High frequency interconnects on silicon substrates," in *IEEE Radio Freq. Integrated Circuit Symp. Dig.*, Denver, CO, 1997, pp. 101–104.

[24] A. C. Reyes *et al.*, "Theoretical and experimental investigation of bias and temperature effects on high resistivity silicon substrates for RF applications," in *IEEE MTT-S Int. Microwave Symp. Dig.*, Baltimore, MD, 1998, pp. 1069–1072.

[25] J. Zheng *et al.*, "CAD-oriented equivalent circuit modeling of on-chip interconnects in CMOS technology," in *7th Topical Meeting Elect. Performance Electron. Packag.*, West Point, NY, Oct. 1998, pp. 227–230.

[26] J. Wee *et al.*, "Modeling the substrate effect in interconnect line characteristics of high-speed VLSI circuits," *IEEE Trans. Microwave Theory Tech.*, vol. 46, pp. 1436–1443, Oct. 1998.

[27] R. E. Collins, *Foundations for Microwave Engineering*. New York: McGraw-Hill, 1992.

Solon J. Spiegel (S'95–A'95) was born in Rio de Janeiro, Brazil, in 1966. He received the B.Sc. degree from the University Gama Filho, Gama Filho, Brazil, in 1989, the M.Sc. degree from the Technion-Israel Institute of Technology, Haifa, Israel, in 1995, and is currently working toward the Ph.D. degree at the Technion-Israel Institute of Technology.

From 1990 to 1992, he was with the Military Institute of Engineering, Rio de Janeiro, Brazil, where he was mainly involved in the areas of GaAs FET characterization and nonlinear analysis of microwave power amplifiers. From 1995 to 1999, he was with the Microwave Group at RAFAEL-The Israel Armament Development Authority, where he was involved in several projects in the area of microwave and millimeter wave modules, MMIC design, and electrical characterization of microwave packages. In 1999, he was involved in the development of high-speed analog-to-digital converters at the IBM Research Laboratory, Haifa, Israel. He is currently with Digital Signal Processing Communications (DSPC), Givat Shmuel, Israel, as a Senior RF Research Member, where he is currently engaged in the development of reconfigurable receivers for dual-mode GSM/W-CDMA applications. His research interests include RF and microwave subsystem integration, modeling and characterization of high-frequency packages, and circuit design for wireless communication systems.

Asher Madjar (S'77–M'79–SM'83–F'97) received the B.Sc. and M.Sc. degrees from the Technion-Israel Institute of Technology, Haifa, Israel, in 1967 and 1969, respectively, and the D.Sc. degree from Washington University, St. Louis, MO, in 1979.

Since 1969, he has been with RAFAEL, Haifa, Israel, and with the Technion-Israel Institute of Technology. While with RAFAEL, he has performed research in the areas of passive and active microwave devices. He headed the Microwave Integrated-Circuit (MIC) Group (1973–1976), and served as a Microwave Chief Engineer in the Communications Department (1979–1982) and Chief Scientist of the Microwave Department (1982 to 1989), with direct responsibility of the MMIC Group (1987–1989). He is currently a Research Fellow involved in microwave optoelectronics activity, MMICs, and monolithic circuits combining microwave and optical devices and microwave modules. At both the Technion-Israel Institute of Technology and the Ort Braude College, he teaches several courses on microwaves, passive microwave devices, active microwave devices, transmission and reception techniques, etc., and serves as an instructor for graduate students. From 1989 to 1991, he was a Visiting Professor at Drexel University, Philadelphia, PA. During that time, he also performed research on optical control of microwave devices and developed a comprehensive model for the optical response of MESFETs. He also participated in graduate student instruction and taught a course on microwave devices. He has authored or co-authored over 100 papers in the areas of microwave components and devices, MICs, MMICs, linear and nonlinear microwave circuits (harmonic balance, APFT, etc.), microwave device modeling (including optical effects), optical links at microwave frequencies, and more.

Dr. Madjar has served as the Israel IEEE Antennas and Propagation Society (IEEE AP-S)/IEEE Microwave Theory and Techniques Society (IEEE MTT-S) chapter chairman for several years, and, in that capacity, organized 13 symposia. From 1985 to 1989, he served as the secretary of the Israel Section of the IEEE. He has also served on the technical committees for MELECON (1981), and the 14th 15th, 16th, 18th, and 19th Electrical and Electronics Engineers Conventions, which were held in Israel. He serves as a member of the Management Committee of the European Microwave Conference since 1990 and as a member of the Technical Program Committee for the European Microwave Conferences since 1993. He served as the chairman of the 27th European Microwave Conference, which was held in Jerusalem, Israel, in September 1997. In April 1996, he was elected to the newly created Steering Committee of the European Microwave Conference. In 1998, he was the recipient of the RAFAEL Best Researcher Prize.